# Structures and Electromagnetic Properties of New Metal-Ordered Manganites; $R$BaMn$_2$O$_6$ ($R$ = Y and Rare Earth Elements)

Tomohiko Nakajima,* Hiroshi Kageyama, and Yutaka Ueda
*Materials Design and Characterization Laboratory,*
*Institute for Solid State Physics, University of Tokyo,*
*5-1-5 Kashiwanoha, Kashiwa, Chiba 277-8581, Japan*

Hideki Yoshizawa
*Neutron Scattering Laboratory, Institute for Solid State Physics,*
*The University of Tokyo, 106-1 Shirakata, Tokai, Ibaraki 319-1106, Japan*

(Dated: February 1, 2008)

New metal-ordered manganites $R$BaMn$_2$O$_6$ have been synthesized and investigated in the structures and electromagnetic properties. $R$BaMn$_2$O$_6$ can be classified into three groups from the structural and electromagnetic properties. The first group ($R$ = La, Pr and Nd) has a metallic ferromagnetic transition, followed by an $A$-type antiferromagnetic transition in PrBaMn$_2$O$_6$. The second group ($R$ = Sm, Eu and Gd) exhibits a charge-order transition, followed by an antiferromagnetic long range ordering. The third group ($R$ = Tb, Dy and Ho) shows successive three phase transitions, the structural, charge/orbital-order and magnetic transitions, as observed in YBaMn$_2$O$_6$. Comparing to the metal-disordered manganites $(R^{3+}_{0.5}A^{2+}_{0.5})$MnO$_3$, two remarkable features can be recognized in $R$BaMn$_2$O$_6$; (1) relatively high charge-order transition temperature and (2) the presence of structural transition above the charge-order temperature in the third group. We propose a possible orbital ordering at the structural transition, that is a possible freezing of the orbital, charge and spin degrees of freedom at the independent temperatures in the third group. These features are closely related to the peculiar structure that the MnO$_2$ square-lattice is sandwiched by the rock-salt layers of two kinds, $R$O and BaO with extremely different lattice-sizes.

PACS numbers:



The magnetic and electrical properties of perovskite-type manganites with the general formula $(R^{3+}_{1-x}A^{2+}_x)$MnO$_3$ ($R$ = rare earth elements and $A$ = alkaline earth elements) have been extensively investigated for the last decade [1]. Among the interesting features are the so-called colossal magnetoresistance (CMR) and metal-insulator (M-I) transition accompanied by charge and orbital ordering. It is now widely accepted that these enchanting phenomena are caused by the strong correlation/competition of multi-degrees of freedom, that is, spin, charge, orbital and lattice.

The structure of perovskite $R$MnO$_3$ consists of MnO$_2$ square-sublattice and $R$O rock-salt-sublattice. The mismatch between the larger MnO$_2$ sublattice and the smaller $R$O sublattice is relaxed by tilting and rotating MnO$_6$ octahedra, leading to the lattice distortion from cubic to, mostly, orthorhombic GdFeO$_3$-type structure. At this lattice distortion, the bond angle $\angle$Mn-O-Mn deviates from 180$^\circ$, resulting in a significant change of an effective one-electron bandwidth ($W$) or equivalently $e_g$-electron transfer interaction ($t$). In the substitution system of $(R^{3+}_{1-x}A^{2+}_x)$MnO$_3$ with a fixed $x$ and a random distribution of $R^{3+}$ and $A^{2+}$, the structural and electromagnetic properties have been explained by the degree of mismatch, that is the tolerance factor $f$ = $(<r_A>+r_{\rm O})/[\sqrt{2}(r_{\rm Mn}+r_{\rm O})]$, where $<r_A>$, $r_{\rm Mn}$ and $r_{\rm O}$ are (averaged) ionic radii for the respective elements, because $W$ or $t$ is changed by varying $f$.

FIG. 1: Generalized phase diagram for $(R^{3+}_{0.5}A^{2+}_{0.5})$MnO$_3$ (Ref. 1). FM: ferromagnetic metal, AFM($A$): $A$-type antiferromagnetic metal, AFI(CE): CE-type antiferromagnetic insulator, COI(CE): CE-type charger/orbital ordered insulator, PM: paramagnetic metal.

Figure 1 shows the generalized phase diagram for $(R^{3+}_{0.5}A^{2+}_{0.5})$MnO$_3$ expressed as a function of $f$[1], where the ferromagnetic metallic (FM) state due to the double-exchange (DE) interaction is dominant near $f \sim 1$ (maximal $W$ or $t$), while the CE-type charge/orbital-ordered (CO) state is most stabilized in the lower $f$ region ($f <$

*e-mail: t-nakaji@issp.u-tokyo.ac.jp

0.975). In the middle region ($f \sim 0.975$), the competition between the ferromagnetic DE and the antiferromagnetic CO interactions results in various phenomena including CMR.

Recently, it has been argued how the $A$-site randomness affect the physical properties of $(R^{3+}_{1-x}A^{2+}_{x})MnO_3$. The phenomena such as the coexistence of FM phase with CO phase and the electronic phase separation [2] may come from the $A$-site randomness. Unfortunately, almost all the works devoted to a series of perovskite-type manganites so far are on the disordered perovskite-type manganites with $R^{3+}$ and $A^{2+}$ ions being randomly distributed. This means that, whenever $x$ is finite, there inevitably exists a disorder in the lattice. Since the physical properties of the manganite perovskite are quite sensitive to even a tiny change in lattice distortion, it is important to employ a compound without $A$-site disorder in order to make clear the effect of $A$-site randomness.

Very recently, we successfully synthesized a metal-ordered perovskite-type manganite $YBaMn_2O_6$ with a successive stacking of YO-$MnO_2$-BaO-$MnO_2$-YO (see Fig. 2(a)) and observed successive three phase transitions; a structural transition without any charge and magnetic order at $T_S$ = 520 K, a CO transition (M-I transition) at $T_{CO}$ = 480 K and an antiferromagnetic transition at $T_N$ = 195 K [3]. The observed $T_{CO}$ = 480 K is the highest among the perovskite-type manganites. Across the phase transition at $T_S$ = 520 K, the resistivity shows little change and the magnetic susceptibility exhibits a large reduction. Furthermore the magnetic interaction seems to be changed from ferromagnetic above $T_S$ to antiferromagnetic below $T_S$. Such transition was first observed in the perovskite manganites. The expectation that such novel transition could be closely related to the metal-ordered structure drove us to the study of metal-ordered perovskite-type manganites $RBaMn_2O_6$. In this paper we report the synthesis, structures and physical properties of new metal-ordered perovskite-type manganites $RBaMn_2O_6$ with a successive stacking of $R$O-$MnO_2$-BaO-$MnO_2$-$R$O. We summarize the results as a phase diagram and we compare the obtained phase diagram with that of $(R^{3+}_{1-x}A^{2+}_{x})MnO_3$ shown in Fig. 1.

Powder samples were prepared by a similar solid-state reaction of $R_2O_3$, $BaCO_3$ and $MnO_2$ to that used for $YBaMn_2O_6$ [3]. The obtained products were checked to be single phases by X-ray diffraction. No perovskite-type compound was produced for Ce, Yb and Lu. The Er- and Tm-compounds included a significant amount of impurity phase.

The crystal structure was determined for 300-573 K by powder X-ray diffraction using CuK$\alpha$ radiation. The superlattice with a charge and orbital ordering was investigated by electron diffraction. The magnetic properties were studied using a SQUID magnetometer in a temperature range $T$ = 5-700 K under a magnetic field of 0.1 T. The electric resistivity of a sintered pellet was measured for $T$ = 100-620 K by a conventional four-probe technique.

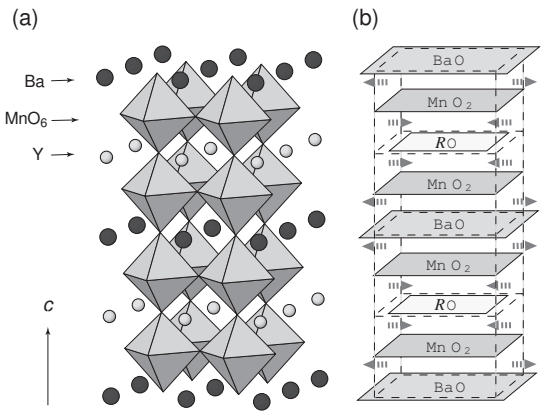


FIG. 2: Crystal structure of $YBaMn_2O_6$ (a) and a schematic illustration of structure for $RBaMn_2O_6$ (b). The $MnO_2$ square-lattice is sandwiched by the rock-salt layers of two kinds, $R$O and BaO with the different lattice-sizes.

The X-ray diffractions of all compounds clearly show the (0,0,1/2)-reflection indexed with the simple cubic perovskite structure, which is an evidence for the same metal-ordered structure as that of $YBaMn_2O_6$. The crystal structure at room temperature is tetragonal ($a_p \times a_p \times 2c_p$) in La- and Pr-compounds, while in the compounds with $R$ = Sm $\sim$ Ho it has a larger cell ($\sqrt{2}a_p \times \sqrt{2}b_p \times 2c_p$) as observed in $YBaMn_2O_6$ [3], where $a_p$, $b_p$ and $c_p$ denote the primitive cell for the simple cubic perovskite. The X-ray diffraction pattern of Nd-compound exhibits a mixture of ($a_p \times a_p \times 2c_p$)- and ($\sqrt{2}a_p \times \sqrt{2}b_p \times 2c_p$)-phases at room temperature.

$RBaMn_2O_6$ can be classified into three groups from the obtained structural and electromagnetic properties. The first group $RBaMn_2O_6$ with $R^{3+}$ = $La^{3+}$, $Pr^{3+}$ and $Nd^{3+}$ has a FM transition at $T_C$, followed by antiferromagnetic transitions in $PrBaMn_2O_6$ (see Fig. 3(a)) and $NdBaMn_2O_6$. The obtained $T_C$ for $LaBaMn_2O_6$ agrees well with the previous report [4]. The neutron magnetic diffraction study has revealed an $A$-type antiferromagnetic transition for $PrBaMn_2O_6$ [5]. This is consistent with the relatively low resistivity below $T_N$ compared with that in the CO state of $EuBaMn_2O_6$ or $DyBaMn_2O_6$, as shown in Fig. 3. A semiconductive behavior in the paramagnetic metallic (PM) state of $PrBaMn_2O_6$ is due to loosely sintered samples. The second group consists of $RBaMn_2O_6$ with $R^{3+}$ = $Sm^{3+}$, $Eu^{3+}$ and $Gd^{3+}$. The compounds exhibit CO transitions, followed by antiferromagnetic long range ordering. Figure 3(b) shows a typical example of magnetic susceptibility and resistivity for $EuBaMn_2O_6$. The third group includes the compounds with $R^{3+}$ = $Tb^{3+}$, $Dy^{3+}$ and $Ho^{3+}$ whose ionic radii are close to $Y^{3+}$. These compounds show three phase transitions as observed in $YBaMn_2O_6$ [3]. The magnetic susceptibility and resistivity of $DyBaMn_2O_6$ are shown in Fig. 3(c) as an example. The distinct transitions at $T_S$, $T_{CO}$ and $T_N$ are commonly observed in this series. The change of magnetic interac-

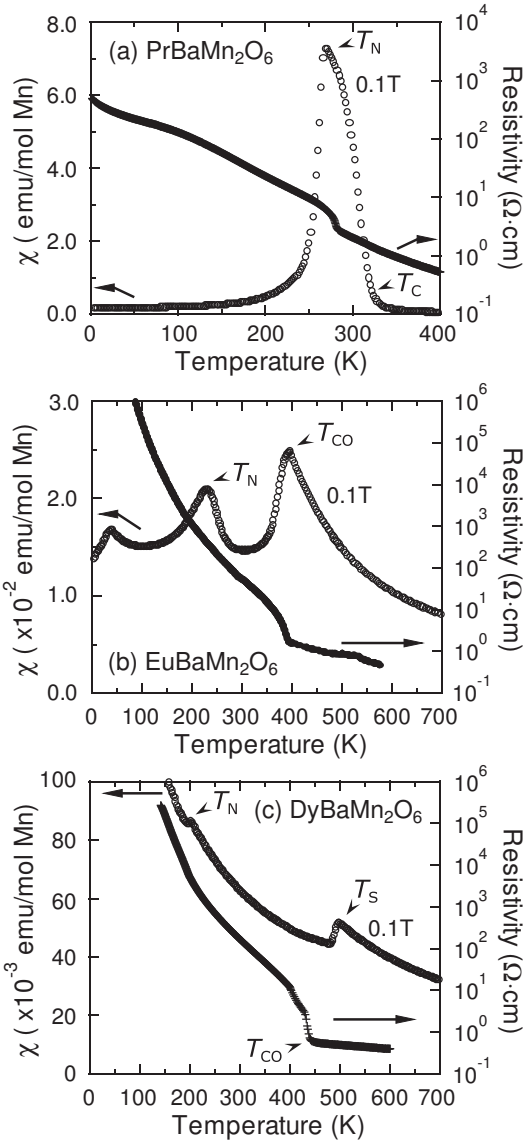


FIG. 3: Temperature dependence of resistivity and magnetic susceptibility ($\chi$) for (a) $PrBaMn_2O_6$, (b) $EuBaMn_2O_6$ and (c) $DyBaMn_2O_6$. $T_C$, $T_N$, and $T_{CO}$ represent the ferromagnetic, antiferromagnetic and charge/orbital-ordered transition temperatures, respectively. $DyBaMn_2O_6$ shows a structural transition without any charge and magnetic order at $T_S$ (see the text).

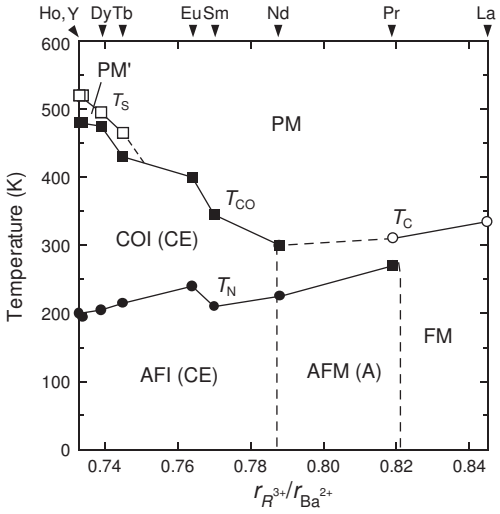


FIG. 4: Phase diagram for $RBaMn_2O_6$. The notation of each phase and transition temperature is the same as that defined in Fig.1 and Fig. 3 (see the text). The PM' is a paramagnetic metal with a possible orbital ordering (see the text). Comparing to the $(R^{3+}_{0.5}A^{2+}_{0.5})MnO_3$, two remarkable features can be recognized in $RBaMn_2O_6$; (1) relatively high $T_{CO}$ and (2) the presence of structural transition at $T_S$ above $T_{CO}$ in $RBaMn_2O_6$ with the small ionic size of $R^{3+}$.

tion from ferromagnetic above $T_S$ to antiferromagnetic below $T_S$ is not so clear in $RBaMn_2O_6$ ($R$ = Tb, Dy, Ho) as in $YBaMn_2O_6$ [3], because of the significant contribution of magnetic rare earth ions to the total magnetic susceptibility. However the reduction of magnetic susceptibility at $T_S$ can be ascribed to a change of Weiss-temperature, namely a change of magnetic interaction, between the PM states above and below $T_S$.

The results are summarized in Fig. 4 as a phase diagram. Here we express the phase diagram as a function of the ratio of ionic radius, $r_{R^{3+}}/r_{Ba^{2+}}$ [6], instead of $f$. In $RBaMn_2O_6$, the $MnO_2$ sub-lattice is sandwiched by the rock-salt layers of two kinds, $R$O and BaO with the different lattice-sizes, as shown in Fig. 2(b) and therefore the tolerance factor cannot be defined. The ratio, $r_{R^{3+}}/r_{Ba^{2+}}$ is a measure of mismatch between $R$O- and BaO-lattices.

It is very interesting to compare Fig. 4 with Fig. 1. Figure 4 is similar to Fig. 1 as a whole. There exist the characteristic phases such as the FM phase and the CE-type CO phase in both phase diagrams. In Fig.1, the FM phase appears in $La_{0.5}Sr_{0.5}MnO_3$ with $f = 0.996$ (the average ionic size of $La^{3+}$(1.36 Å)/$Sr^{2+}$(1.44 Å) = 1.40 Å). In Fig.4, on the other hand, the FM phase appears around $R$ = La and the CO state becomes dominant for Nd and later rare earth. Incidentally if a hypothetical tolerance factor $f$' were calculated from the average ionic size of $R^{3+}/Ba^{2+}$, the FM phase would appear around $f$' = 1.026 ($LaBaMn_2O_6$) far beyond $f$' = 1 and the CO phase would be stable around $f$' = 1 (from $f$' = 1.005 for $SmBaMn_2O_6$ to $f$' = 0.995 for $YBaMn_2O_6$). In $RBaMn_2O_6$, the $MnO_2$ sub-lattice is sandwiched by $R$O and BaO layers with the different lattice-sizes and as a result the $MnO_6$ octahedron itself is distorted in a peculiar manner that the oxygen atoms of $MnO_2$ square-lattice are strongly bound by $R^{3+}$ resulting in a buckling of Mn and oxygen atoms in the $MnO_2$ square plane [7], in contrast to the rigid $MnO_6$ octahedra in $(R^{3+}_{0.5}A^{2+}_{0.5})MnO_3$. The ionic size of $Ba^{2+}$ (1.61 Å) [6] is much larger than those of $Sr^{2+}$ and all of $R^{3+}$. In the combination of $R^{3+}/Ba^{2+}$ the mismatch between $R$O- and BaO-lattices

is the smallest in $La^{3+}/Ba^{2+}$. Therefore lattice distortion is expected to be a little in $LaBaMn_2O_6$. Actually the structure of $LaBaMn_2O_6$ is tetragonal and the FM phase appears as the ground state. Here it should be noticed again that $PrBaMn_2O_6$ with the second smallest mismatch shows the FM to $A$-type antiferromagnetic metal (AFM) transition. A similar $A$-type AFM transition was previously reported in metal-disordered $Pr_{0.5}Sr_{0.5}MnO_3$ or $Nd_{0.5}Sr_{0.5}MnO_3$ with $f \sim 0.985$ [8]. Among the FM phases the $T_C$ is little dependent of the ratio, $r_{R^{3+}}/r_{Ba^{2+}}$. This suggests that the lattice distortion in $RBaMn_2O_6$ is not so considerable as the ferromagnetic interaction or DE interaction is influenced. Actually the Weiss temperature in the PM region above $T_S$ is a ferromagnetic value about +300 K even in $YBaMn_2O_6$ which has the largest lattice distortion. On the other hand, the CO state becomes stable as the ratio, $r_{R^{3+}}/r_{Ba^{2+}}$ decreases. The $T_{CO}$ increases across $T_C$ around $NdBaMn_2O_6$ and reaches the champion record $T_{CO} = 480$ K in $YBaMn_2O_6$. Our recent study of electron diffraction and neutron diffraction has revealed that $YBaMn_2O_6$ has a CE-type charge and orbital order with a 4-fold periodicity along the $c$-axis ($2\sqrt{2}a_p \times \sqrt{2}b_p \times 4c_p$) [9]. Taking the layer-type metal-order into the consideration, this new type of charge and orbital order (4-CE-type CO) can be explained as follows: the orbital ordered pattern within the $a$-$b$ plane varies in the phase across the BaO- or YO-layer, that is $\alpha\alpha\beta\beta$-stacking along the $c$-axis, where the $\beta$-type is derived from the interconversion of the $d_{3x^2-r^2}$- and $d_{3y^2-r^2}$-sublattices in the ordinary CE-type layer ($\alpha$-type).

There are remarkable features in the phase diagram of $RBaMn_2O_6$; (1) the high $T_{CO}$ and (2) the presence of structural transition at $T_S$ above $T_{CO}$. It is easy to understand the relatively high $T_{CO}$ in $RBaMn_2O_6$, because the absence of randomness at $A$-site and the layer-type metal-order are favorable for the charge ordering of $Mn^{3+}/Mn^{4+}$. Furthermore the phase diagram indicates that the increase of the mismatch between $R$O- and BaO-lattices also enhances the charge ordering. The structural transition at $T_S$ is not accompanied by any charge and magnetic order but by the reduction of magnetic susceptibility. The temperature dependences of magnetic susceptibility suggest the change of magnetic interaction with Mn ions from ferromagnetic above $T_S$ to antiferromagnetic below $T_S$ [3]. Such novel transition is characteristic of the compounds with small ionic radii of $R^{3+}$ in which the $MnO_2$ square-lattice is sandwiched by two rock-salt layers with extremely different lattice-sizes. This situation introduces a strong frustration to the $MnO_2$ sub-lattice and as a result the $MnO_6$ octahedron itself is heavily distorted leading to a complex structural deformation (triclinic or monoclinic) [7]. Such deformation must give a new perturbation to the competition of multi-degrees of freedom among charge, orbital, spin and lattice, and affect the characteristic properties such as CMR and charge/orbital ordering. We propose a possible orbital ordering, presumably $d_{x^2-y^2}$-type orbital ordering, at $T_S$, referring to the $A$-type AFM. We have obtained some evidence for the orbital ordering from the detailed structural investigation by X-ray and neutron diffraction [7]. The freezing of the orbital, charge and spin degrees of freedom at the independent temperatures, $T_S$, $T_{CO}$ and $T_N$, could be closely related to the peculiar structure of the metal-ordered perovskite-type manganites, that is a layer type and a low symmetric structure, an asymmetric distortion of $MnO_6$ octahedron and so on.

In the phase diagram of $(R^{3+}_{0.5}A^{2+}_{0.5})MnO_3$, the middle region ($f \sim 0.975$) where the ferromagnetic DE and the antiferromagnetic CO interactions compete each other is responsible for various phenomena including CMR. Such region may correspond to the solid solution between $NdBaMn_2O_6$ and $SmBaMn_2O_6$ or $PrBaMn_2O_6$ in the phase diagram of $RBaMn_2O_6$. Actually rather complex behaviors have been observed in $NdBaMn_2O_6$ [5]. Furthermore our preliminary experiments have revealed the successful synthesis of metal-disordered manganites $(R^{3+}_{0.5}Ba^{2+}_{0.5})MnO_3$. The $(R^{3+}_{0.5}Ba^{2+}_{0.5})MnO_3$ will give us a chance of quantitative discussion on the effect of $A$-site randomness.

In summary, new metal-ordered perovskite-type manganites $RBaMn_2O_6$ ($R$= Y and rare earth elements) have been synthesized and investigated in the structures and electromagnetic properties. The $RBaMn_2O_6$ can be classified into three groups from the obtained structural and electromagnetic properties. The first group ($R$ = La, Pr and Nd) has a metallic ferromagnetic transition, followed by an $A$-type antiferromagnetic transition in $PrBaMn_2O_6$. The second group ($R$ = Sm, Eu and Gd) exhibits a CO transition, followed by an antiferromagnetic long range ordering. The third group ($R$ = Tb, Dy and Ho) shows successive three phase transitions, the structural, CO and magnetic transitions, as observed in $YBaMn_2O_6$. Comparing to metal-disordered $(R^{3+}_{0.5}A^{2+}_{0.5})MnO_3$, there are two remarkable features in $RBaMn_2O_6$; (1) the relatively high charge-order transition temperature and (2) the presence of structural transition without any charge and magnetic order above the charge order temperature in the third group. We propose a possible orbital ordering at the structural transition, that is a possible freezing of the orbital, charge and spin degrees of freedom at the independent temperatures in the third group. These are closely related to the structural feature that the $MnO_2$ sub-lattice is sandwiched by two kinds of rock-salt layers, $R$O and BaO with the different lattice-sizes and as a result the $MO_6$ octahedron itself is distorted in a peculiar manner.

The authors thank T. Yamauchi, M. Isobe, T. Matsushita, Z. Hiroi and H. Fukuyama for valuable discussion. This work is partly supported by Grants-in-Aid for Scientific Research (No. 407 and No. 758) and for Creative Scientific Research (No. 13NP0201) from the Ministry of Education, Culture, Sports, Science, and Technology.

## References

[1] See for reviews: C. N. R. Rao and B. Raveau, *Colossal*

*Magnetoresistance, Charge Ordering and Related Properties of Manganese Oxides*; World Scientific, Singapore (1998).
[2] S. Mori, C. H. Chen, and S-W. Cheong, Phys. Rev. Lett. **81** (1998) 3972.
[3] T. Nakajima, H. Kageyama and Y. Ueda, J. Phys. Chem. Solids **63** (2002) 913.
[4] F. Millange, V. Caignaert, B. Domengès, and B. Raveau, Chem. Mater. **10** (1998) 1974.
[5] in preparation
[6] R. D. Shannon, Acta Crystallogr. A **32** (1976) 751.
[7] T. Nakajima *et al.*, submitted to J. Solid State Chemistry.
[8] H. Kawano, R. Kajimoto, H. Yoshizawa, Y. Tomioka, H. Kuwahara and Y. Tokura, Phys. Rev. Lett. **78** (1997) 4253.
[9] H. Kageyama *et al.*, submitted to J. Phys. Soc. Japan.